The Journal of Experimental Biology 211, 3009-3019
Published by The Company of Biologists 2008
doi:10.1242/jeb.018895

Consequences of buoyancy to the maneuvering capabilities of a foot-propelled aquatic predator, the great cormorant (*Phalcrocorax carbo sinensis*)

Gal Ribak[1,*], Daniel Weihs[2] and Zeev Arad[1]

[1]Department of Biology and [2]Faculty of Aerospace engineering, Technion, Haifa 32000, Israel

*Author for correspondence at present address: Department of Biology, University of South Dakota, Vermillion, SD 57069, USA (e-mail: gal.ribak@gmail.com)

Accepted 20 June 2008

SUMMARY

Great cormorants are foot-propelled aquatic divers utilizing a region of the water column where their underwater foraging behavior is affected by their buoyancy. While swimming horizontally underwater, cormorants use downward lift forces generated by their body and tail to overcome their buoyancy. Here we assess the potential of this swimming strategy for controlling maneuvers in the vertical plane. We recorded the birds swimming through a submerged obstacle course and analyzed their maneuvers. The birds reduced swimming speed by only 12% to maneuver and were able to turn upward and then downward in the sagittal plane at a minimal turning radius of 32±4 cm (40% body length). Using a quasi-steady approach, we estimated the time-line for hydrodynamic forces and the force-moments produced while maneuvering. We found that the tail is responsible for the pitch of the body while motions of the body, tail, neck and feet generate forces normal (vertically) to the swimming direction that interact with buoyancy to change the birds' trajectory. Vertical maneuvers in cormorants are asymmetric in energy cost. When turning upward, the birds use their buoyancy but they must work harder to turn downward. Lift forces generated by the body were always directed ventrally. Propulsion improves the ability to make tight turns when the center of the turn is ventral to the birds. The neck produced only a small portion (10%) of the normal vertical forces but its length may allow prey capture at the end of pursuit, within the minimum turning radius.

Key words: maneuverability, locomotion, swimming, diving, torque, pitch, trim-control.

INTRODUCTION

Efficient underwater locomotion should include the ability of the swimmer to control its trajectory and maneuver when necessary. For cormorants swimming underwater in search and pursuit of their motile prey (fish), the ability to make abrupt maneuvers while swimming is equally as important as the ability to swim faster than their prey. Maneuverability is broadly defined as the opposite of stability, i.e. the responsiveness of the body to deviate from a steady trajectory (Fish, 2002; Webb, 2002; Weihs, 1993; Weihs, 2002). The term maneuver describes unsteady aspects of motion and can also be used to describe changes in swimming speed without a change in swimming direction (i.e. accelerating and braking). However, here, we refer exclusively to the ability and limits of making a controlled change to the swimming direction. Turning involves accelerating normal to the instantaneous direction of swimming. Since this centripetal acceleration is a function of tangential speed and trajectory radius these two parameters have been widely used to characterize the maneuvering performance of various swimmers (e.g. Blake et al., 1995; Fish, 2002; Fish and Nicastro, 2003; Fish et al., 2003a; Rivera et al., 2006; Walker, 2000). However, these two parameters *per se* cannot explain how animals control their maneuvers or highlight the factors limiting maneuverability. To obtain such insights, one must explore how the organism maneuvers (e.g. Fish and Nicastro, 2003; Webb and Weihs, 1983). In the present study, we report on the hydrodynamic mechanism used by cormorants to maneuver in the vertical plane.

Cormorants are foot-propelled aquatic predators that rely exclusively on submerged swimming for capturing fish (Johnsgard, 1993). They are extremely efficient aquatic predators, reportedly yielding some of the highest catch per unit effort recorded for avian divers (Grémillet et al., 2001). They achieve this remarkable foraging performance despite a limited adaptation for a pelagic life style. Like several other avian divers, cormorants utilize the aquatic media while retaining full flight capabilities. The primary adaptation of the avian body for flight results in low specific density. Underwater this translates into avian divers being among the most buoyant pelagic swimmers (Lovvorn and Jones, 2004; Wilson et al., 1992). The high buoyancy is due to the light skeletons of birds and the large air volumes carried underwater inside the body (air sacs) and trapped in the plumage. Enstipp et al. showed that the energy expenditure of swimming cormorants changes with dive depth (Enstipp et al., 2006). Water depth provides relief from buoyancy to deep divers by compressing the air volumes in the body. However, great cormorants seldom dive to depths exceeding 10 m (Grémillet et al., 1999). As a result, they forage in the part of the water column where their swimming is affected by their positive buoyancy. Understanding how cormorants cope with their buoyancy to maneuver efficiently underwater is an important step for a better understanding of the foraging behavior and habitat selection (e.g. preferred foraging depth) in these aquatic predators.

Cormorants use foot-propulsion for swimming underwater. During swimming, the wings are folded next to the body and do not participate in swimming (Johnsgard, 1993). As a result, the body of cormorants is deprived of median control surfaces that are used for trim-control in many fish and marine mammals (Fish, 2002; Fish and Shannahan, 2000; Webb and Weihs, 1983). While swimming horizontally in a straight line, cormorants do so with their body inclined (pitch) at a negative angle-of-attack (AoA) to the

swimming direction. This produces hydrodynamic lift forces that are directed downward and help the bird overcome its buoyancy while swimming horizontally (Ribak et al., 2004; Ribak et al., 2006). The angles of the body and tail alternate during the paddling cycle, suggesting that the birds are using their flat tails as hydrofoils to regulate the pitch angle of the body. By tilting it independently from the body, the tail can generate lift from the motion of the bird through the water, and the resulting moment can be used to pitch the body and control its cyclic rotation through the paddling cycle. The angle of the body, in turn, can regulate the lift forces produced by the body and the tail. When their buoyancy was artificially reduced by attaching weights to the body, cormorants swimming in a straight horizontal trajectory reduced their body angle to reduce the vertical forces produced during swimming (Ribak et al., 2006). This suggests that the birds can regulate the dynamic forces produced during swimming to achieve equilibrium of forces with changing buoyancy in the vertical axis. Since the dynamic forces are a result of the swimming speed of the birds, the birds may require a minimum swimming speed to maintain such an equilibrium. However, cormorants need to do more than swim in a straight horizontal line, and by controlling the magnitude of vertical forces the birds may be able to control their trajectory. How they actually do this is demonstrated in the present study.

We report on an experiment designed to explore the mechanism for pitch control and vertical maneuvering in shallow-swimming great cormorants. Since the birds actively resist buoyancy during swimming we hypothesized that maneuvers in the vertical plane will involve shifting the equilibrium of the normal forces produced during swimming with buoyancy to result in a net normal force in the desired direction. Since the normal forces produced during swimming are hydrodynamic and derived from the swimming speed of the birds, we expected the birds to maintain a minimal swimming speed throughout the maneuver for generating sufficient lift by the body and tail. The inability of the birds to slow down would result in a limit to the maneuvering capabilities (turning radius). To test these ideas experimentally, we constructed a submerged obstacle course that forced the birds to perform a vertical maneuver by swimming in a bell-shaped trajectory. We tested the maneuvering limitation of the birds by progressively increasing the difficulty of the obstacle course. The swimming of the birds through the obstacle course was filmed and analyzed to reveal how the birds control their trajectory and orientation.

MATERIALS AND METHODS

Experimental set-up

We used four female and four male great cormorants (*Phalcrocorax carbo sinensis* Blumelbach 1798). All were adults (i.e. >2 years) at the time of the experiment. Six of the birds were hand-reared in captivity since hatching while the other two (a male and a female) were wild birds captured under permit. Holding facilities and the experiments were approved by the Technion Committee for Supervision of Animal Experimentations (permit No. IL-080-11-2001). The birds are the same individuals that were used in previous studies of horizontal swimming (Ribak et al., 2004; Ribak et al., 2005; Ribak et al., 2006) and were housed in the same aviary and pool described therein. Hence, only a brief description of the facilities is provided below.

The birds were trained to enter a pool (8×5 m, 1 m deep) one at a time and dive from one end of the pool to the other through a 7 m-long, submerged enclosure ('channel') with a rectangular cross section (0.5×0.5m) made of metal fencing (mesh size, 0.02×0.05 m). The channel was placed on the bottom of the pool. Starting 3.5 m away from the entrance to the channel, a 2 m-long section of the channel was used as the test section. It was filmed from the side using submerged video camera that covered the section and a 45 deg. inclined mirror placed above the section. The mirror provided an upper view of the channel. The birds were motivated to dive through the channel by rewarding them with fish at one end. At the time of the experiment, the birds were familiar with the channel and the pool and were routinely diving from one side of the channel to the other as part of their weekly training protocol conducted for over one year. For the experiment reported in the present study, we altered the channel described above by adding thin, 0.25 m-high vertical barriers made of the same metal mesh as the channel. The barriers were put in place to block the passage through the upper or lower half of the tunnel (Fig. 1). At the center of the test section one barrier ($B_{0.5}$) was placed to block the passage through the lower half of the tunnel. Two additional barriers were placed at equal distances along the channel length on either side of $B_{0.5}$ (B_0 towards the entrance and B_1 towards the exit). B_0 and B_1 blocked the passage through the upper half of the channel. Two additional barriers were placed further towards the entrance to the channel, also blocking the upper half of the channel, to ensure that the birds reached B_0 after swimming in the lower half of the channel.

In order to pass through this obstacle course, the birds needed to swim horizontally for 3.5 m in the lower half of the channel, pass beneath B_0, swim up to the upper half of the channel, pass over

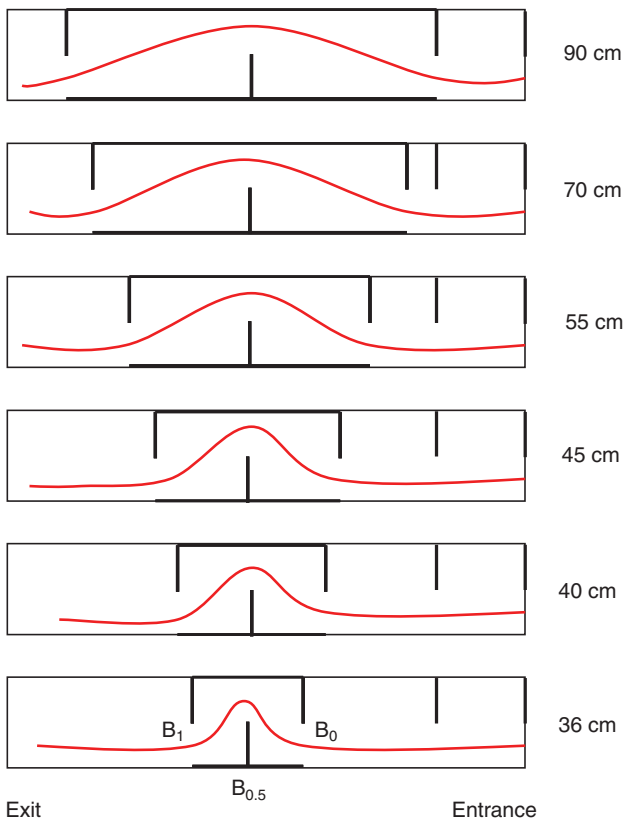

Fig. 1. A diagram of the different levels of the obstacle course used to establish the maneuvering capabilities of cormorants. The numbers on the right are the horizontal distances between adjacent barriers (thick vertical lines). The vertical barrier in the center of all levels is $B_{0.5}$ (see text), which was kept at a fixed position inside the channel. The two neighboring barriers that were moved closer between trials are B_0 and B_1, respectively. The red line represents the trajectory of the birds through the course.

$B_{0.5}$, swim down to the lower half of the channel, straighten horizontally and finally pass beneath B_1. As a result, the birds were changing their swimming direction three times in alternating directions, thus forming a bell-shaped trajectory through the obstacle course (Fig. 1). The first and third turns have the center of the turn above the bird and the second turn had the center of the turn below the bird. We first placed B_0 and B_1 1.0 m on either side of $B_{0.5}$ and allowed the birds to familiarize with the changes to the channel until they were all navigating between the barriers smoothly and repeatedly. The distance of B_0 and B_1 from $B_{0.5}$ was then progressively reduced. At each change in distance between the hurdles, the birds were allowed two days of training to swim through the course. Once all birds had routinely passed the course without touching the barriers, a further 1 to 2 days were dedicated to filming the birds in the obstacle course. The distance between the barriers was then progressively reduced and the same procedure was repeated.

We filmed the birds swimming through the obstacle course (one at a time) at six difficulty levels when the horizontal distance between the barriers was 90, 70, 55, 45, 40 and 36 cm. Each bird was filmed swimming through the channel several times. We discarded sequences in which the birds were seen to touch any of the barriers. In the remaining sequences we measured the duration (number of video fields, 50 fields s^{-1}) of when the tip of the bill passed beneath B_0 to the time when the tip of the tail passed beneath B_1. The shortest sequence for each bird in each maneuvering level was used for further analysis as it represented the maximum performance for that bird at that maneuvering level. In these sequences, for each video field, we digitized the positions (Fig. 2): of the tip of the tail (P1); the base of the tail (P2); a marker (a 1.5 cm-diameter circle divided by its radii into six equal areas with alternate colors of red and yellow printed on a 2×2 cm yellow adhesive tape), which was glued (SuperWiz, Loctite; Rocky Hill, Connecticut, USA) to the wing feathers, approximating the position of the center of mass (Ribak et al., 2004) along the major axis of the body (P3); the point between the neck and body (P4); the tip of the bill (P5); the base of the foot (P6); and the tip of the longest digit (P7). Additionally, five points between P4 and P5 were digitized in sequence (N1–N5) from the neck to the bill. They did not correspond to specific landmarks on the neck but were all placed on the mid-line of the neck and head as observed in the images. All the points described above were digitized in the side view of the birds. In the upper view (through the mirror), we only digitized the tip of the bill (P5), the point of connection between the neck and body (P4) and the tip of the tail (P1) for calibration purposes (distance from the camera) and to ensure that no significant lateral perturbation of the body, neck or tail was evident in the movies.

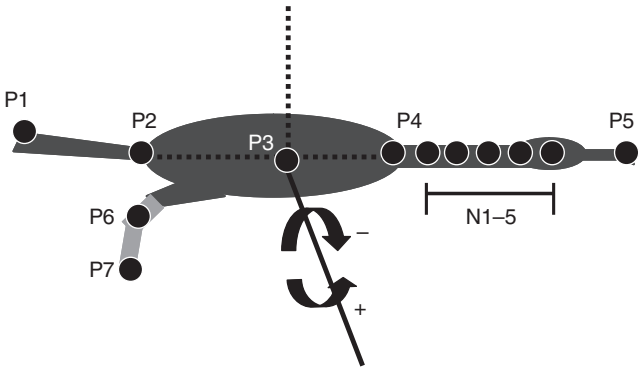

Fig. 2. A representation of the body of cormorants illustrating the points on the body that were digitized in the side-view video (see text for details). Axes depicted on the body with a broken line represent the morphological horizontal and vertical axes. The solid line represents the lateral axis and is shown here to illustrate the terminology used to describe rotations and moments in the vertical plane (pitch).

Motion analysis from video

All analysis was performed in 2-D, focusing only on the vertical plane where the trajectory of the birds occurred. The horizontal axis (x) was chosen parallel to the length of the channel, with positive values increasing in the horizontal direction of swimming. The vertical axis (y) was positive in the direction pointing upward. The walls of the tunnel prevented the birds from having a lateral component of motion, thus justifying the 2-D approach. We used the marker point on the body to calculate the swimming speed and trajectory of the birds from the videos. Swimming speed was calculated from the change in position of the center of mass (P3) along the horizontal and vertical axes between fields (time) using numerical derivation [four points parabola approximation (Rayner and Aldridge, 1985)]. A second time derivative provided the acceleration. The components of velocity were used to trigonometrically calculate the instantaneous swimming direction, and the velocity and acceleration components were used to calculate the instantaneous turning radius (R) from the curvature (k_{xy}) of the trajectory of the birds in the vertical plane:

$$|R| = k_{xy}^{-1} = \frac{(u_x^2 + u_y^2)^{1.5}}{(u_x a_y - u_y a_x)} , \quad (1)$$

where the subscripts x and y refer to the horizontal and vertical speeds (u, m s^{-1}) and accelerations (a, m s^{-2}). k_{xy} denotes the direction of turning according to the right-hand rule (here, positive when the center of the turn is above the bird). Hence, the bell-shaped trajectory resulted in values of positive curvature as the birds entered and exited the obstacle course and negative values at the center of the obstacle course. Since the center of the maneuver represented the tightest turn (Fig. 1), the turning radius for each bird in each maneuvering difficulty level was calculated by averaging only the values (from Eqn 1) with negative curvature. Mean swimming speed for each bird in each difficulty level of the obstacle course was obtained by calculating the mean of the instantaneous speeds between the time points (video fields) where P3 passed beneath B_0 and B_1. The coordinates of points P1 with P2 and points P2 with P4 were used to calculate the pitch angle (relative to the horizontal) of the tail (α_T) and body (α_B), respectively. α_B was numerically derived with respect to time (as described above for swimming speed) to obtain the angular velocity and angular acceleration of the body. As for the data for the turning radius, we calculated the mean angular velocity of the body for each maneuvering difficulty level only when the values were negative corresponding to the nose-down rotation at the center of the obstacle course. The coordinates of points P4 and P5 provided a robust description of the pitch angle of the neck (α_N). A more accurate description accounting for the flexibility of the neck is provided below also using points N1–N5 (see estimation of forces).

To compare the swimming of the birds at the different levels of maneuvers we used a non-dimensional axis where the x-axis for each difficulty level was adjusted so that the position of $B_{0.5}$ was assigned a value of 0.5 (arbitrary units) and B_0 and B_1 were 0 and 1.0, respectively. As a result, the adjusted axes represent the

horizontal position inside the obstacle course relative to the barriers rather than the actual position.

The fields in which the birds were observed paddling were noted during the analysis. We considered birds to be paddling in fields where the foot was seen to move backwards and up relative to the body. Throughout this work variation among the eight birds is reported as ± s.d.

Estimation of forces

We previously estimated the vertical forces produced by the body, tail and feet of cormorants during straight horizontal swimming using a quasi-steady approach and technical data taken from published wind tunnel studies on geometrical shapes (Ribak et al., 2004). Whenever possible we followed the same estimation method here. However, several adjustments were required for the more complex case of swimming in a curved path. We therefore describe in detail the points differing from our previous analysis (Ribak et al., 2004) and only mention briefly the methods adopted from our original study.

Usually, during straight, horizontal swimming the neck is stretched forward and the head points in the swimming direction (Ribak et al., 2004). However, this was not the case when the birds maneuvered. We therefore modeled the contribution of the neck and head to the forces and moments used for turning. To account for the bending of the long, flexible neck during maneuvers we used the digitized data from points P4, P5 and N1–5. For each time step (video field), we used these seven points as nodes to interpolate (using cubic-spline.) 24 equally spaced points representing 23 cross sections along the neck and head. This allowed us to treat the neck flexibility by modeling it as a sum of 23 finite elements, each oriented differently with respect to the flow. The most anterior section corresponds to the pointed tip of the bill and consequently was not included in the estimation. For each of the remaining 22 elements we calculated the instantaneous velocity from the distance moved between fields as described above. Each section was assumed to be a fixed length cylinder (l=1.5 cm) aligned with the length of the neck. The angle of the length of each section relative to the direction of velocity of the section is the angle-of-attack of the section (α). Each section was assigned a different diameter (d) based on actual diameters measured from a cormorant neck in fig. 1 in Ribak et al. (Ribak et al., 2005). To model the hydrodynamic forces produced by each section we used the cross-flow principle (Hoerner, 1965). A cylinder with its length inclined with respect to the flow at an angle α produces a hydrodynamic force normal to the length of the cylinder (F_N). This force can be estimated as:

$$F_N = \tfrac{1}{2}(\rho l d C_N u^2) \quad (2)$$

and

$$C_N = C_D \sin^2\alpha, \quad (3)$$

where ρ is water density (1000 kg m^{-3}) and u is speed. C_D is the drag coefficient of the cylinder (based on frontal area) when the cylinder is oriented normal to the direction of flow. We used C_D=1.1 as in fig. 18, p. 3–11 in (Hoerner, 1965).

The normal forces from all 22 neck sections were combined using vector summation to give the total force generated by the neck. Because we were interested in how the birds control their maneuvers we also summed the moments generated by each neck section. The moment generated by the i-th neck section was estimated as the cross product of the 2-D vector connecting P3 to the i-th neck section ($\mathbf{r_i}$) and $\mathbf{F_{Ni}}$. The moment ($\mathbf{M}$) generated by the neck was calculated by summing the moments of the different sections:

$$\mathbf{M} = \sum_i \mathbf{r_i} \times \mathbf{F_{Ni}}, \quad (4)$$

where positive moments correspond to nose-up pitching and negative moments correspond to nose-down torque. The moment estimation method knowingly overlooks the fact that the center of mass can shift slightly forwards and backwards as the neck moves with respect to the body. This minor inaccuracy is not expected to affect the insights from this analysis.

For the hydrodynamic forces generated by the tail, we previously used an approximation to a delta-shaped hydrofoil experiencing flow deflected by the body (Ribak et al., 2004). In a subsequent study (Ribak et al., 2006), we noted that this is a good approximation only when the body and tail are at small AoA (<15 deg.), as in the case of rapid swimming in a straight line. When the birds were swimming more slowly, they tilted their body further, exposing parts of the tail directly to the free stream flow (Ribak et al., 2005; Ribak et al., 2006). Consequently, in the present study where the birds were forced to slow down and were tested on their ability to rotate their body within the maneuver, we considered the tail as a delta-shaped hydrofoil experiencing flow from its motion relative to the water, independent of the wake of the body. We took the center of the dynamic pressure of the tail to be located at 0.6 of the distance between the base of the tail and tip of the tail, as suggested by the delta wing model (Hoerner and Borst, 1985). The instantaneous position of this hydrodynamic center was used to calculate the velocity of this point in the videos as described above. The geometric AoA of the tail was calculated from α_T and the direction of velocity of the tail. We calculated the C_L and C_D coefficients for the tail from the leading-edge-suction analogy (Polhamus, 1971). This calculation requires only the measured AoA of the tail and coefficients for the potential flow (k_p=1.3) and vortex lift (k_v=3.15) that are obtained from charts [fig. 3 in Polhamus (Polhamus, 1968)] based on aspect-ratio of the tail [AR=1.0 (Ribak et al., 2004)].

The C_L and C_D coefficients of a thin delta wing with sharp edges are then calculated as:

$$C_L = (k_p \sin\alpha\cos^2\alpha) + (k_v \cos\alpha\sin^2\alpha), \quad (5)$$

$$C_D = C_L \tan\alpha. \quad (6)$$

The lift (L) and drag (D) forces are obtained by multiplying the calculated coefficients by the dynamic pressure:

$$L = \tfrac{1}{2}(\rho^4 A C_L u^2), \quad (7)$$

$$D = \tfrac{1}{2}(\rho A C_D u^2). \quad (8)$$

where A is the area of the tail [A=0.0073 m^2 (Ribak et al., 2004)]. We were then able to calculate the resultant force vector for the tail, which acts at the center of pressure of the tail. From the force vector and the distance between the center of pressure and P3, we calculated the turning moment that the tail exerts on the body, similar to Eqn 4.

For the lift forces produced by the tilted body we used the same estimation method described previously (Ribak et al., 2004). Lift is calculated using Eqn 7, where the C_L is taken from the AoA of the body (α) and wind tunnel data on streamlined bodies (C_L=0.008α). C_L is based on a characteristic area (A=0.0225 m^2), which is the square of the maximum width (left to right) of the body. As we were primarily interested in forces with a component normal to the swimming direction that can be used for maneuvering, we did not need to calculate the drag of the body, which, by definition, is in the direction of swimming. Drag and lift generated

by the body can contribute to pitching the body when the hydrodynamic center of the body is anterior or posterior to the center of mass. As there are no data to indicate otherwise, we assume here that in cormorants the hydrodynamic center is close enough to the center of mass, thus resulting in zero pitch.

Finally, since the birds paddled at all of the maneuver levels, we also added the contribution of thrust generated by the feet during the stroke phase using the same estimation approach described previously (Ribak et al., 2004). The thrust of the feet is assumed to be the vector sum of lift, drag and inertia (acceleration reaction, including the virtual mass of the feet). The estimation of force assumes that the feet function as a low aspect-ratio (AR=4), thin hydrofoil moving at an arch beneath the body at speed, acceleration and AoA derived from the kinematics of points P6 and P7 in the video. This estimation, based on a 2-D view, ignores lateral forces that should cancel out due to the symmetry of synchronized strokes where both feet paddle together at the same time. We also disregarded any forces that might be introduced by the feet during the recovery phase of the paddling cycle when the webbed toes are adducted.

To elucidate the mechanism of maneuvering and to test whether the forces calculated are realistic we summed the contribution of the different body parts to the forces normal to the instantaneous direction of swimming. We then compared this sum with the centrifugal force and the component of buoyancy that a 2 kg bird (the mean body mass of the birds used) would encounter while moving in the bell-shaped trajectory inside the obstacle course. Buoyancy estimates (B=2.3 N kg^{-1}) were based on empirical measurements from carcasses reported previously (Ribak et al., 2004). The component of buoyancy that is normal to the swimming direction (Bsin β, where β is the angle between the direction of buoyancy and the direction of swimming velocity) was added to the centrifugal force (F_{cg}), which acts normal to the direction of swimming. The centrifugal force was calculated as:

$$F_{cg} = -ma_c, \quad (9)$$

where m is the mass of the bird and a_c is the instantaneous centripetal acceleration during the maneuver, calculated as:

$$a_c = u^2/R, \quad (10)$$

where u is the instantaneous swimming speed and and R is the turning radius. R is calculated from Eqn 1, and the minus sign in Eqn 9 implies that the force is directed opposite to the a_c (outside of the turn).

RESULTS

We progressively decreased the horizontal distance between the barriers in the obstacle course down to 0.34 m, at which point the birds were not capable of repeatedly passing thorough the course without touching the barriers despite 3 days of repeated attempts. We therefore concluded that the difficulty level prior to this trial (when the barriers were 0.36 m apart) represents the maximum maneuvering capability for great cormorants for this particular type of maneuver. The mean turning radius of the birds when they were swimming through the course with the barriers 0.36 m apart was 0.32±0.04 m (Fig. 3). The mean turning radius decreased during the different trials. Fig. 4 shows the mean swimming speed of the birds while passing through the obstacle course. The birds were swimming significantly faster in the two easiest levels of the experiment (wider maneuvers, 0.9 and 0.7 m), then reduced their speed [repeated-measure analysis of variance (ANOVA), P<0.001] by 12% on average (range 7–27%).

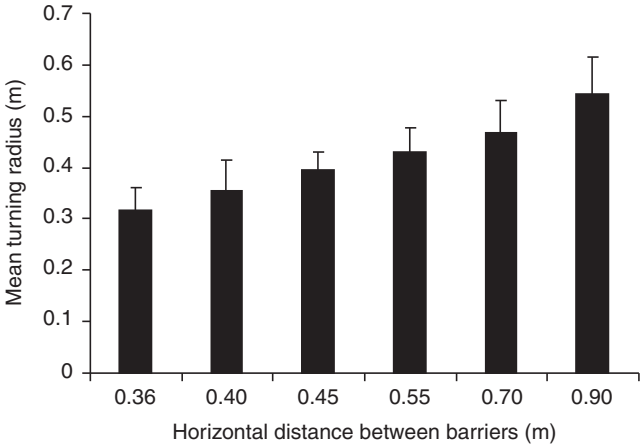

Fig. 3. Mean ± s.d. (N=8) of the observed turning radius for each maneuvering level. The data are for the center of the maneuver when the birds are passing above $B_{0.5}$ (see Materials and methods for further details).

Swimming speeds during the four tighter maneuver levels did not differ from each other (Tukey post-hoc, P>0.9). The higher swimming speeds for the wider maneuvers were not different (Tukey Post-Hoc, P>0.68) from the mean speeds measured using the same birds during a previous study [table 2 in Ribak et al. (Ribak et al., 2005)], where the birds were swimming through the same channel but with no vertical barriers (no maneuvers). Table 1 summarizes some of the observed differences in maneuvering kinematics between the different maneuver levels. At the tightest maneuver, the instantaneous a_c peaked when the bird was above $B_{0.5}$, reaching values of >1.5 $\boldsymbol{g}$ (where $\boldsymbol{g}$ is gravity). Fig. 5 shows the change in pitch angle (relative to the horizon) of the body, neck and tail as the birds passed through the obstacle course. Pitch angles oscillated while the birds were passing through the obstacle course but there was a phase shift between the three body parts (tail, body and neck). As a result, the neck and tail were deflected relative to the angle of the body (Fig. 6). The interesting point to note in Fig. 6 is that the birds are moving their tail and neck relative to their body in a similar manner in all of the maneuvering difficulty

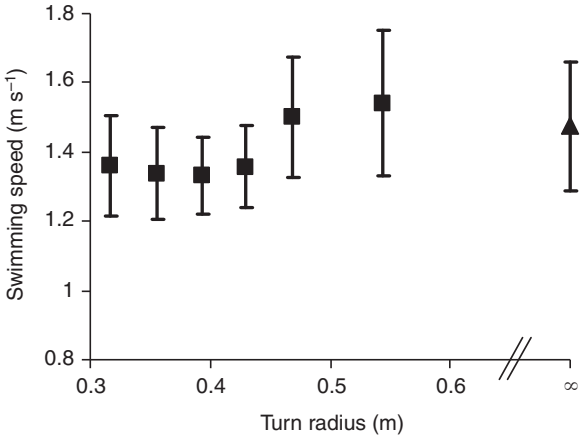

Fig. 4. Mean ± s.d. swimming speeds of the great cormorant (N=8) inside the obstacle course. Data are plotted as a function of the mean turning radius in each difficulty level (see Fig. 3). Squares denote the present study on vertical maneuvers. The triangle denotes data from Ribak et al. (Ribak et al., 2005) for the same birds during unobstructed swimming in a straight line (turning radius=∞).

Table 1. Observed maneuvering parameters in the various levels of the obstacle course

Horizontal distance between barriers (m)	Mean angular speed of the body (deg. s^{-1})	Mean centripetal acceleration ($m\,s^{-2}$)	Maximum centripetal acceleration/g^*
0.90	97±16.5	5.5±0.81	1.14±0.346
0.70	130±12.6	5.8±1.06	1.28±0.193
0.55	159±22.1	5.5±0.34	1.32±0.297
0.45	199±38.8	5.7±0.84	1.28±0.177
0.40	204±41.7	6.8±1.14	1.55±0.299
0.36	269±51.6	7.5±1.59	1.58±0.353

Data are means ± s.d. from eight birds. Each bird in each level was represented by the fastest trial. The data are averaged from the center of the obstacle course, where curvature of the birds was negative (see Materials and methods section for explanation). Maximum centripetal force is reported in a non-dimensional form by dividing it by gravity. *g=9.8 $m\,s^{-2}$.

levels but the amplitude of the motions increases as the maneuver becomes tighter.

In most cases, the birds were observed to paddle three times in each of the video sequences. The first stroke was typically before B_0. The second stroke was performed between the two outer barriers in the vicinity of $B_{0.5}$, and the third stroke was either before or after the birds passed beneath B_1. However, there was high variability among the birds, and within the actions of individual birds, especially in the tighter turns. It seemed that the birds tended not to paddle near B_0 (Fig. 7). In a few cases, the birds seemed to slow down the recovery phase between the first and second stroke, which might have helped them to slow down before reaching $B_{0.5}$; however, this observation was not consistent in all the birds or trials.

Fig. 8 shows the calculated moments generated by the neck and tail. Since the birds only changed the amplitude of the tail and neck pitch between the different maneuvering levels, only the data for the tightest maneuver are shown to minimize redundancy. The moments of the neck and tail are mirror images of one another, implying that they work in opposite directions most of the time. However, the moments generated by the tail are an order of magnitude larger than the moments generated by the neck. As a result, the observed rotation of the body (angular acceleration) correlates with the pitching moment of the tail. Fig. 9 shows the component of forces generated by the body tail and neck that are directed normal (in the sagittal plane) to the instantaneous swimming direction of the body. The data are means from all of the birds, and only the mean for the tightest maneuver is shown. The body contributes forces that are always directed ventrally; the tail and neck can generate forces directed dorsally but the contribution of the neck is minor compared with the forces produced by the body and tail. Fig. 10 summarizes the net force normal to the direction of swimming calculated for each bird by summing the contribution of the body, tail, neck and propulsion of the feet. Also shown are the component of buoyancy in the direction normal to the swimming direction and the centrifugal force calculated for a bird with a body mass of 2 kg. It can be seen that in the first and last third of the maneuver, where the birds' buoyancy and centrifugal force have opposite directions, the forces produced by the birds are lower while at the second third, where buoyancy and the centrifugal force have the same direction, the forces produced by the birds are much higher, mostly due to the contribution from foot propulsion (compare Fig. 10 with Fig. 9).

DISCUSSION

The aim of the experiment described in the present study was to determine the submerged, vertical maneuvering capabilities and to reveal the mechanism employed by cormorants to control their trajectory underwater. The results show that cormorants use a complex array of synchronized motions by different body parts to adjust their trajectory. While the rotation of the body in the vertical plane is predominantly regulated by the tail, the normal forces responsible for changing the direction of swimming are a combined action of the feet, tail, body and neck. The birds regulate these forces by adjusting the AoA of the body, tail and neck and timing propulsion to specific locations inside the obstacle course. Regulating the contribution of the different body parts allows the birds to achieve zero net normal force (equilibrium) during swimming in a straight line or to shift the equilibrium in one direction in order to maneuver.

We chose to focus on vertical rather than horizontal maneuvers and on bell-shaped maneuvers rather than simple turns for three reasons. First, cormorants are foot-propelled divers powered by their webbed feet, which are located posterior and ventral to the center of mass of the body. This results in a cyclic body pitching during each paddling cycle where the stroke is performed when the body is at maximum pitch (Ribak et al., 2004). Cormorants use the lift from their body to resist their buoyancy and direct thrust vertically. This swimming strategy seems well adapted for buoyant divers needing to swim horizontally underwater. However, foraging is not limited to horizontal trajectories and the asymmetry of foot propulsion in cormorants (in the dorsoventral axis) raises the question of how the birds control their trajectory when large pitch angles are needed to maneuver in the vertical plane? The bell-shaped, vertical trajectory reveals the birds' ability to control their trajectory by forcing them to alternate swimming direction between both sides of the body (ventral and dorsal) as well as to regulate the magnitude of the forces and moments produced during swimming. We elaborate further on this asymmetry below.

The second reason for focusing on vertical maneuvers has to do with swimming stability. When thrust is produced posterior to the center of mass, swimming is unstable because a slight perturbation causing the center of mass to deviate from the line of action of thrust (e.g. a sudden pitch) will result in a larger torque, further increasing the perturbation (Weihs, 2002). By contrast, when thrust is produced anterior to the center of mass the design is stable and perturbations will subside passively. Wing-propelled birds have their wings close to the center of mass, resulting in a more stable trim-control. Many fish and marine mammals generate thrust posterior to the center of mass but they also posses fins anterior to the center of mass that can stabilize the pitch of the body (Fish, 2000; Webb and Weihs, 1983). Cormorants do not have such stabilizers, and the only horizontal surface is the tail that is posterior to the body. The maneuver described here enables the evaluation of the function of the tail as a pitch control device by comparing the motions of the tail with the angular acceleration of the body.

More importantly, the bell-shaped maneuver allows distinction between the pitch control function of the tail and the heave (normal

acceleration) function. Fig. 9 shows that when the bird is between B_0 and $B_{0.5}$ the tail produces a normal force directed above the trajectory of the bird. This force is correlated with a negative moment generated by the tail and a change in direction of the angular acceleration of the body (clockwise) but not with the requirements for normal force equilibrium, which would suggest a negative force (Fig. 10). Thus, the bell-shaped maneuver provides evidence to support our hypothesis that the predominant function of the tail is probably pitch control.

The third reason is that understanding pitch control in cormorants is also fundamental for horizontal turning. Videos of cormorants performing 90 deg. horizontal turns show that the birds roll their body in order to perform banked turns, with the ventral side of the birds facing the center of the turn. Thus, for horizontal sideways turns, the birds are rolling to pitch the body as they turn. Although in the present study, we report only on the maneuvering of the birds in the vertical plane the insights are relevant for maneuvering in general.

For buoyant cormorants, any swimming direction other than vertical results in a component of buoyancy that is out of plane relative to the swimming direction. If the birds stop actively swimming, their trajectory will change due to the unbalanced action of buoyancy. Hence, because of buoyancy the swimming of cormorants is inherently unstable in the vertical plane. This has an implication for maneuvering that does not exist in neutrally buoyant swimmers. Vertical maneuvers in great cormorants are not symmetrical. Fig. 10 shows that the forces required to change swimming direction by a few degrees upwards are not the same as the forces required to make the same change downwards. The estimation of forces produced by the birds at different stages of the maneuver show that during the first third of the maneuver the birds changed their swimming direction almost passively by relaxing the forces resisting buoyancy and allowing buoyancy to divert

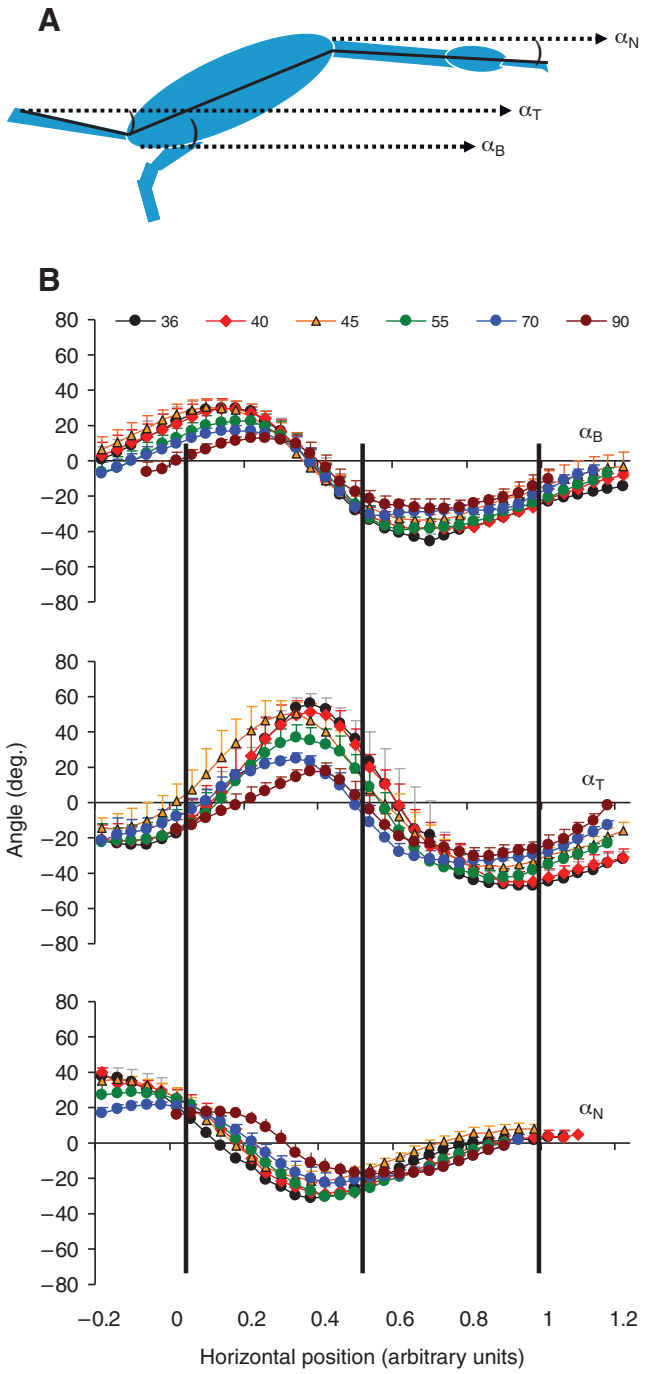

Fig. 5. Mean pitch angles of the body (α_B), tail (α_T) and neck (α_N) as a function of position of the bird (N=8) inside the obstacle course. (A) Figure of the bird illustrating the different angles. Angles below the horizontal are considered negative. In the graphs each symbol represents the different level of difficulty of the obstacle course. The number in the legend denotes the horizontal distances (cm) between vertical barriers (Fig. 1). The horizontal axis was normalized by dividing it by the distance between the two extreme barriers and shifting the horizontal position of the first barrier to zero. As a result the vertical barriers overlap in all of the maneuvering levels (vertical black lines). Error bars are ± s.d.

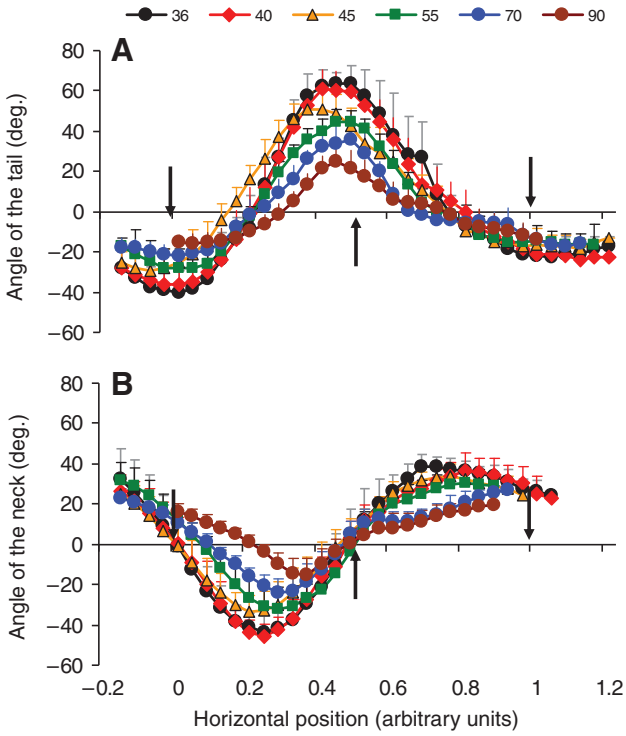

Fig. 6. Mean pitch angle of the tail (A) and neck (B) relative the long axis of the body of the birds (N=8) as a function of the position of the birds inside the obstacle course. Different symbols denote the different difficulty levels of the obstacle course. The legend describes these levels as the horizontal distance between adjacent barriers (cm) (Fig. 1). Vertical arrows denote the position of the barriers. The horizontal axis was normalized by dividing it by the distance between the two extreme barriers and shifting the horizontal position of the first barrier to zero. Error bars are ± s.d.

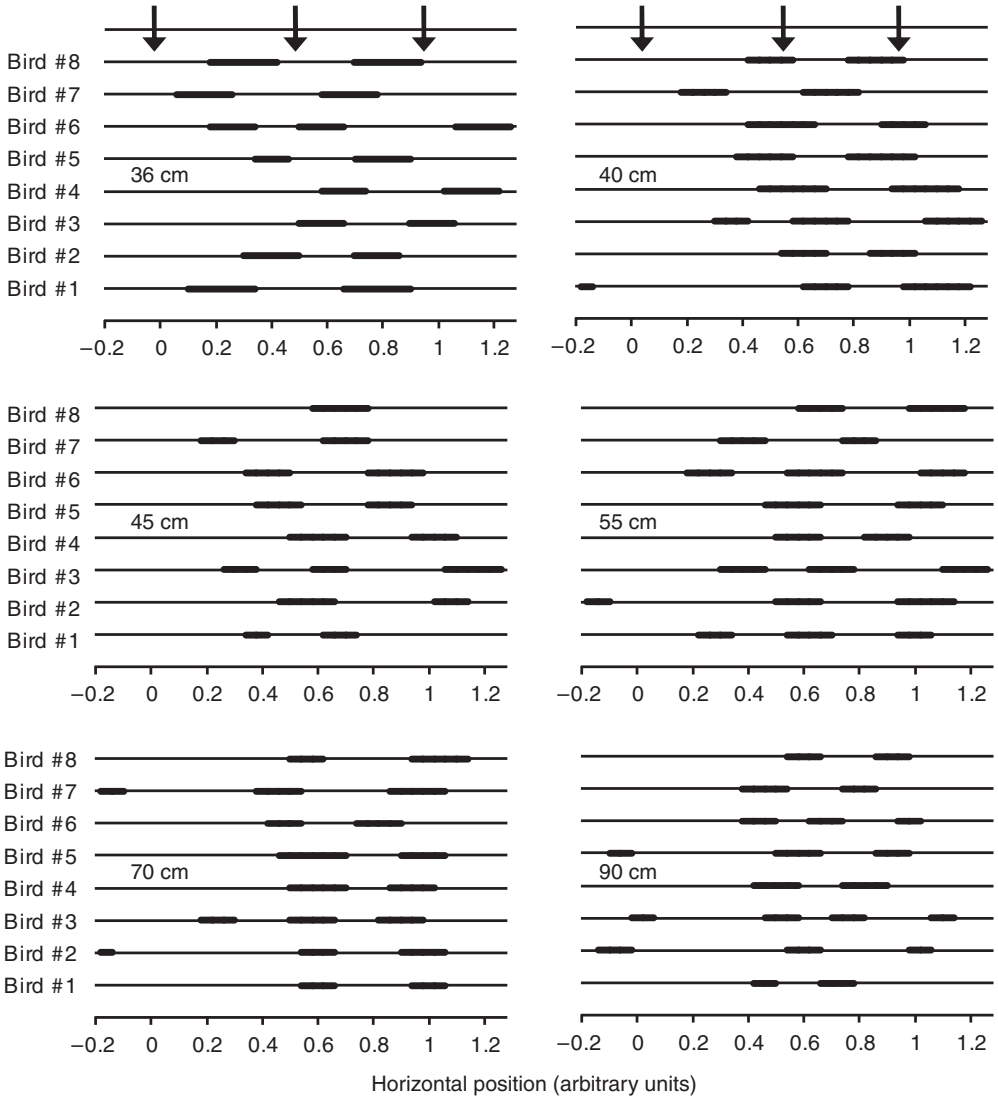

Fig. 7. Occurrence of foot propulsion as a function of position inside the obstacle course. Each chart represents a maneuvering difficulty level labeled according to the horizontal distance between the adjacent barriers (cm) (Fig. 1). Black bars denote the adjusted horizontal positions within the obstacle course where active paddling (stroke) was observed in the video. Note that the birds are less likely to paddle while entering the obstacle course (horizontal axis=0) and more likely to paddle above the second barrier (horizontal axis=0.5). Vertical arrows denote the positions of the barriers (0, 0.5 and 1.0) on the adjusted horizontal axis.

them upwards. In the second third of the maneuver the birds were producing the highest normal forces to stop their acceleration upwards and convert the trajectory of the body downwards against buoyancy. It was at this stage that the birds tended to paddle the most.

Vertical maneuvers are asymmetric not just because of the direction of buoyancy. The body of the birds is asymmetrical in the dorso–ventral axis and the feet of cormorants are ventral to the body. We previously estimated that the thrust produced by the feet of cormorants during shallow horizontal swimming is equally directed forward and down (Ribak et al., 2004). Thus, much of the propulsive force can be used to produce a downwards curved swimming direction but this is associated with a nose-up pitching moment generated by the feet. Indeed, cormorants swimming in a constant direction have a slightly undulating trajectory where the swimming direction is curved downwards during the active phase of the paddling cycle and curves up during the passive (recovery and glide) phase. At the same time, the oscillating pitch of the body is adjusted so that the stroke starts when the body is at maximum pitch. This undulation during horizontal swimming seems to be regulated by the tail (Ribak et al., 2004). While maneuvering, the asymmetry in propulsive force can imply that the birds that were performing a tight maneuver with their ventral side inside the turn may not be able to replicate such a tight maneuver if the barriers were changed to invert the bell-shaped trajectory, forcing the birds to make a tight turn with their dorsal side facing into the turn. Thus, tight maneuvers in cormorants are probably active (i.e. the birds paddle throughout the maneuver) not only to maintain swimming speed but also to contribute normal forces for one-sided (ventral to the bird) vertical maneuvering. Figs 9 and 10 show that without foot propulsion the normal forces produced by the body and tail would only be half of the requirement for a downward-directed curved trajectory needed above $B_{0.5}$.

Our experiment shows that the birds reduced their swimming speed by only 12% between unobstructed swimming and the tightest maneuver possible. When evaluating this observation it should be noted that we used a gradual experimental design in which the difficulty level (trials) of the obstacle course increased in correlation with trial order. This was done to test the maximum maneuvering capabilities of the birds. In theory such a gradual design has the potential of incorporating gradual learning into the results. To eliminate this potential we allowed the birds to train at each difficulty level for two days prior to the measurement. This training ensured that the birds were already familiar with the course at the time of measurement.

The reason that the birds hardly reduced their swimming speed is likely to be a consequence of the mechanism employed by cormorants to maneuver. To change the direction of swimming the

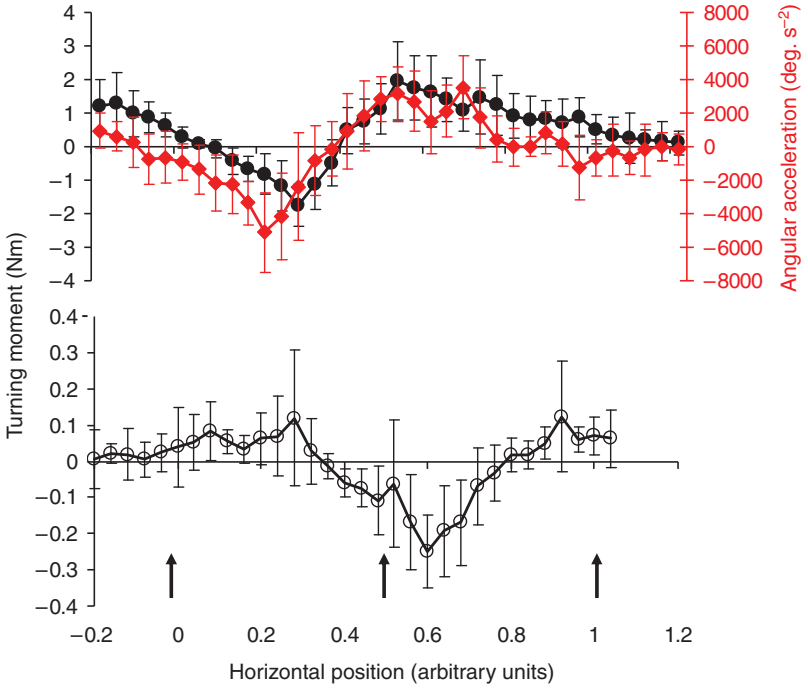

Fig. 8. The turning moments generated by the tail (solid black circles) and neck (open circles) as a function of the birds' position inside the obstacle course. The data are means ± s.d. from eight birds passing through the obstacle course at the highest difficulty level (0.36 m between the barriers, Fig. 1). Note the order of magnitude difference in the scale of the vertical axes. Red symbols are the angular acceleration of the body, which correlates with the moment of the tail. Vertical arrows denote the position of the vertical barriers. The horizontal axis is the same as in Figs 5–7 to allow equivalent evaluation.

birds must produce a centripetal acceleration with a magnitude proportional to the square of swimming speed and inversely proportional to the turning radius (Eqn 10). As the birds perform a tighter maneuver, the turning radius will decrease and the required centripetal acceleration will increase unless the speed is reduced further. For great cormorants foraging at shallow depth, slowing down is not an option. Except for the thrust produced by the feet, all the normal hydrodynamic forces are derived from the swimming speed of the body. If the birds slow down, the normal turning force needed to change the swimming trajectory will decrease but so will the normal forces produced by the birds. The birds are probably reluctant to swim at lower speeds because the normal hydrodynamic forces produced would be too small to allow them precise control over their swimming direction. The combined action of the hydrodynamic forces with buoyancy to determine the dynamic equilibrium of the forces, dictates that a minimum level of normal force is required for controlled swimming. Since this minimum force is hydrodynamic and derived from the speed of the body, the birds have a minimal speed limitation for controlled swimming. This minimal swimming speed results in a minimum turning radius setting a limit to maneuvering in a tight space.

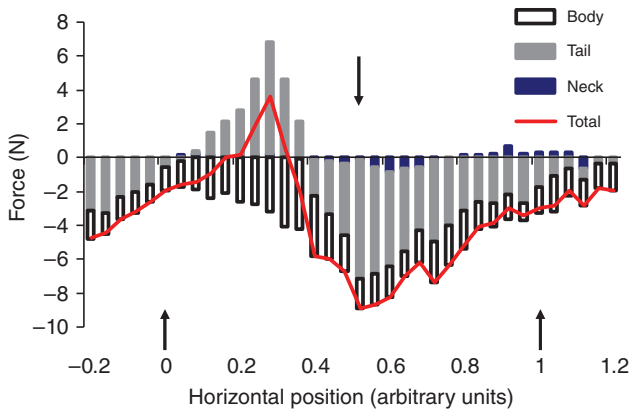

Fig. 9. The forces produced normal to the swimming direction as a function of the position inside the obstacle course. The forces are produced by the body, tail and neck moving at an angle of incidence to the flow. The columns are means of the forces from eight birds passing through the obstacle course at the highest difficulty level (0.36 m between barriers, see Fig. 1). The red line is the sum of the three forces. Positive values are directed dorsally, and negative values are directed ventrally. Vertical arrows denote the position of the barriers. The horizontal axis is the same as in Figs 5–8 to allow equivalent evaluation.

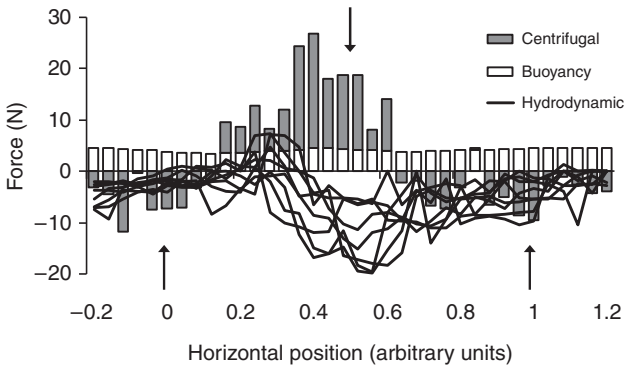

Fig. 10. Normal forces during vertical maneuvers of great cormorants as a function of the position inside the obstacle course. Each black line is the net normal force generated by a single bird (out of N=8 birds). The net force is calculated by summing the forces normal to the instantaneous swimming direction from the motion of the body, tail, neck and foot propulsion. The forces are calculated for the birds passing through the obstacle course at the highest difficulty level (0.36 m between barriers, see Fig. 1). Filled and open columns denote centrifugal force and the component of buoyancy that is normal to the swimming direction, respectively. These forces are estimated based a mean body mass of 2 kg and the average instantaneous swimming speed, swimming direction and turning radius (see text). All forces are positive when they are directed above the bird's trajectory and negative when they are directed below it. The vertical arrows point to the position of the barriers on the adjusted horizontal axis. The horizontal axis is the same as in Figs 5–9 to allow equivalent evaluation.

The long and flexible neck of cormorants may be an adaptation to overcome such a limitation. Undoubtedly, the neck has additional functions, such as in head stabilization for vision, but the ability to move a neck that is as long as the body independently of the body can help the bird catch an escaping fish. The minimal turning radius found in the present study was, on average 32 cm. The length of the neck plus the head of a great cormorant reaches 40% of the total length of the body or ~0.34 m for a 0.85 m-long bird [fig. 1 in Ribak et al. (Ribak et al., 2005)]. The close similarity between the length of the neck and the minimum turning radius means that the length of the cormorant neck is just enough to capture small prey that could otherwise outmaneuver the larger and faster cormorant. Smaller more maneuverable prey can find refuge from a faster and larger predator by escaping into the 'inner circle of safety' defined by the minimum radius of turning of the predator, which is proportional to the body mass and therefore much larger than that of the smaller prey (Howland, 1974; Weihs and Webb, 1984). The long neck of the cormorant can allow the predator to reach into this inner circle and intercept the prey. Such capability would be a great advantage for a predator that must keep a fast swimming speed underwater.

In theory, the long and flexible neck of cormorants could also have a hydrodynamic function. It should be noted that a 34 cm-long cylinder with a mean diameter of 3 cm, moving through the water at 1.35 m s^{-1} (Fig. 4), with its long axis perpendicular to the flow, can generate a hydrodynamic force as high as 10 N. This force is twice as high as the estimate for buoyancy of great cormorants at 1 m depth used in the present study. This force would also be high compared with the normal forces estimated for the body and tail (Fig. 9). However, in our experiment the birds were seen to make very little use of this option. Normal forces produced by the neck only peaked at ~1 N (Fig. 9). The neck is flexible so that it can follow the curved trajectory during a maneuver and generate minimal drag. By allowing the neck to deviate slightly from this trajectory, the neck can move at an AoA producing forces normal to its length. During the experiment, the birds were seen to bend their neck considerably while maneuvering. The measured AoA of the different neck sections was not necessarily small but these angles changed along the neck so that positive AoA in sections close to one end of the neck were negative for sections closer to the other end of the neck. Hydrodynamic forces produced by the neck as a whole were smaller than the potential according to the AoA of individual neck sections because the forces from different sections of the neck tended to cancel each other out. Thus, much of the hydrodynamic forces produced by the neck were 'wasted' as drag. This can be a consequence of the tight, bell-shaped trajectory where the anterior section of the neck and head were moving in front of the body, with the trajectory curving downwards while the posterior section of the neck and the body were still following a path curving upwards. For simple turns in one direction the neck function can be more unidirectional and substantial. However, there is a more compelling explanation as to why the neck is not used extensively for vertical maneuvers. The tail generates a substantial portion of the hydrodynamic forces used for turning and also controls the body orientation (pitch). If both the tail and neck produce forces in the same direction, the moments produced by the tail posterior to the body and by the neck anterior to the body will have opposite signs and work against each other. Since the body needs to rotate during the maneuver, the contribution of the neck to the forces available for turning cannot be so high as to interfere with rotation of the body during the maneuver.

Fig. 4 can be used to represent the maneuvering capabilities of cormorants when maneuvering is defined as the standardized minimal turning radius (in body lengths) for a standardized swimming speed (body lengths s^{-1}). An average cormorant with a body length of ~85 cm can turn at a radius of 0.38 body length while swimming at a speed of 1.6 body lengths s^{-1}. We were unable to find comparable data for vertical maneuvers in other swimming organisms. However, the vertical maneuverability of cormorants (as defined above) matches the highest values of horizontal maneuverability (side turns) recorded in cetaceans (i.e. at a swimming speed of 1.6 body lengths s^{-1}, cormorants can make tighter turns than most cetaceans) [see fig. 7 in Fish (Fish, 2002)]. This result is probably a consequence of the long and flexible neck of cormorants, which 'inflates' body length compared to mass of the body, thus reducing the standardized turning radius. The vertical maneuverability of cormorants also matches values of horizontal maneuverability recorded from two species of sea lions. However, the sea lions were capable of making slower turns at a much smaller turning radius [~0.1 body lengths, California sea lion: fig. 1 in Fish et al. (Fish et al., 2003a); Steller sea lion, fig. 6 in Cheneval et al. (Cheneval et al., 2007)]. Sea lions are highly flexible semi-aquatic predators actively seeking and chasing fish at structurally complex locations (Fish et al., 2003a). As such, their maneuverability might be more similar to cormorants, which utilize the aquatic environment solely for foraging whereas cetaceans are also designed for stability during open water swimming at low energetic cost (Fish, 2002; Fish et al., 2003b).

In the transition to foraging in water, aquatic birds diverged into two aquatic strategies. Some aquatic birds use their wings for swimming underwater while others use their feet. The occurrence of both strategies shows that both are successful. Evolution of wing-propelled divers focused on solving the required dynamic scaling of wing propulsion to efficiently operate in both water and air (Lovvorn et al., 1999). By contrast foot-propelled birds separate propulsion between water and air and can, therefore, remain specific for propulsion in each medium. However, the present study reveals that the separation between locomotion in water and air in foot-propelled cormorants requires a separate maneuvering mechanism for each medium and therefore the development of a specific pitch-control mechanism for motion underwater. Such a mechanism comes at a price of elevated drag from the pitched body (Ribak et al., 2005). This suggests that cormorants are not designed for swimming underwater at minimal energetic cost but rather are designed to match the dynamic lifestyle of aquatic predators adapted for fast, maneuverable swimming in the realm of positive buoyancy.

LIST OF ABBREVIATIONS

a_c	centripetal acceleration
a_x	instantaneous horizontal acceleration
a_y	instantaneous vertical acceleration
A	area
AR	aspect ratio
B	buoyancy
B_0	first vertical barrier in the obstacle course
$B_{0.5}$	second vertical barrier in the obstacle course
B_1	third vertical barrier in the obstacle course
C_D	drag coefficient
C_L	lift coefficient
C_N	normal force coefficient
d	diameter of cylinder
D	hydrodynamic drag
F_{cg}	centrifugal force
F_N	hydrodynamic force normal to the length of a cylinder inclined to the flow
F_{Ni}	the normal hydrodynamic force generated by the i-th neck segment
k_p	potential flow coefficient for a delta-shaped wing

k_v	vortex lift coefficient for a delta-shaped wing
k_{xy}	instantaneous curvature of the trajectory in the vertical plane
l	length of a cylinder
L	hydrodynamic lift
m	body mass
M	pitching moment
r_i	the vector connecting the i-th neck segment to the center of mass
R	instantaneous turning radius
u	swimming speed
u_x	instantaneous horizontal swimming speed
u_y	instantaneous vertical swimming speed
α	angle-of-attack (AoA)
α_B	pitch angle of the body relative to the horizontal axis
α_N	pitch angle of the neck relative to the horizontal axis
α_T	pitch angle of the tail relative to the horizontal axis
β	angle between the swimming direction and buoyancy
ρ	water density

The authors wish to thank R. Almon, T. Mordechay, E. Maor and T. Eviatar-Ribak for assistance in training, animal care, experiments and movie analysis, and the VPR Fund for Promotion of Research (to D.W.) for partial support.

REFERENCES

Blake, R. W., Chatters, L. M. and Domenici, P. (1995). Turning radius of yellowfin tuna (*Thunnus albacares*) in unsteady swimming maneuvers. *J. Fish Biol.* **46**, 536-538.

Cheneval, O., Blake, R. W., Trites, A. W. and Chan, K. H. S. (2007). Turning maneuvers in Steller sea lions (*Eumatopias jubatus*) *Mar. Mamm. Sci.* **23**, 94-109.

Enstipp, M. R., Grémillet, D. and Jones, D. R. (2006). The effect of depth, temperature and food ingestion on the foraging energetics of a diving endotherm, the double-crested cormorant (*Phalacrocorax auritus*). *J. Exp. Biol.* **209**, 845-859.

Fish, F. E. (2002). Balancing requirements of stability and maneuverability in cetaceans. *Integr. Comp. Biol.* **42**, 85-93.

Fish, F. E. and Nicastro, A. J. (2003). Aquatic turning performance by the whirligig beetle: constraints on maneuverability by a rigid biological system. *J. Exp. Biol.* **206**, 1649-1656.

Fish, F. E. and Shannahan, L. D. (2000). The role of pectoral fins in body trim in sharks. *J. Fish Biol.* **56**, 1062-1073.

Fish, F. E., Hurley, J. and Costa, D. P. (2003a). Maneuverability by the sealion *Zalophus californianus*: turning performance of an unstable body design. *J. Exp. Biol.* **206**, 667-674.

Fish, F. E., Peacock, J. E. and Rohr, J. J. (2003b). Stabilization mechanism in swimming odantocete cetaceans by phased movements. *Mar. Mamm. Sci.* **19**, 515-528.

Grémillet, D., Wilson, R. P., Storch, S. and Gary, Y. (1999). Three-dimensional space utilization by a marine predator. *Mar. Ecol. Prog. Ser.* **183**, 263-273.

Grémillet, D., Wanless, S., Carss, D. N., Linton, D., Harris, M. P., Speakman, J. R. and Le Maho, Y. (2001). Foraging energetics of arctic cormorants and the evolution of diving birds. *Ecol. Lett.* **4**, 180-184.

Hoerner, S. F. (1965). *Fluid-Dynamic Drag*. Bakersfield: Hoerner Fluid Dynamics.

Hoerner, S. F. and Borst, H. V. (1985). *Fluid-Dynamic Lift*. Bakersfield: Hoerner Fluid Dynamics.

Howland, H. C. (1974). Optimal strategies for predator avoidance: the relative importance of speed and manoeuverability. *J. Theor. Biol.* **47**, 333-350.

Johnsgard, P. A. (1993). *Cormorants, Darters and Pelicans of the World*. Washington: Smithsonian Press.

Lovvorn, J. R. and Jones, D. R. (1994). Biomechanical conflicts between adaptation for diving and aerial flight in estuarine birds. *Estuaries* **17**, 62-75.

Lovvorn, J. R., Croll, D. A. and Liggins, G. A. (1999). Mechanical versus physiological determinants of swimming speeds in diving Brunnich's guillemots. *J. Exp. Biol.* **202**, 1741-1752.

Polhamus, E. C. (1968). Application of the leading-edge-suction analogy to the vortex lift to the drag due to lift of sharp-edge delta wings. *NASA Tech. Memo.* D-4739.

Polhamus, E. C. (1971). Predictions of the vortex-lift characteristics by a leading-edge-suction analogy. *J. Aircr.* **8**, 193-199.

Rayner, J. M. V. and Aldridge, H. D. J. (1985). Three-dimensional reconstruction of animal flight paths and the turning flight of microchiropteran bats. *J. Exp. Biol.* **118**, 247-265.

Ribak, G., Weihs, D. and Arad, Z. (2004). How do cormorants counter buoyancy during submerged swimming? *J. Exp. Biol.* **207**, 2101-2114.

Ribak, G., Weihs, D. and Arad, Z. (2005). Submerged swimming of the great cormorant *Phalacrocorax carbo sinensis* is a variant of the burst and glide gait. *J. Exp. Biol.* **208**, 3835-3849.

Ribak, G., Klein, N., Weihs, D. and Arad, Z. (2006). Adjustment of submerged swimming to changes in buoyancy in cormorants. *Can. J. Zool.* **84**, 383-396.

Rivera, G., Rivera, A. R. V., Dougherty, E. E. and Blob, R. W. (2006). Aquatic turning performance of painted turtles (*Chrysemys picta*) and functional consequences of a rigid body design. *J. Exp. Biol.* **209**, 4203-4213.

Walker, J. A. (2000). Does a rigid body limit maneuverability? *J. Exp. Biol.* **203**, 3391-3396.

Webb, P. W. (2002). Control of posture, depth and swimming trajectories of fishes. *J. Integ. Comp. Biol.* **42**, 94-101.

Webb, P. W. and Weihs, D. (1983). *Fish Biomechanics*. New York: Praeger.

Weihs, D. (1993). Stability of aquatic animal locomotion. *Contemp. Math.* **141**, 443-461.

Weihs, D. (2002). Stability versus maneuverability in aquatic locomotion. *J. Integ. Comp. Biol.* **42**, 127-137.

Weihs, D. and Webb, P. W. (1984). Optimal avoidance and evasion tactics in predator–prey interactions. *J. Theor. Biol.* **106**, 189-206.

Wilson, R. P., Hustler, K., Ryan, P. G., Burger, A. E. and Noldeke, E. C. (1992). Diving birds in cold water: do Archimedes and Boyle determine energetic costs? *Am. Nat.* **140**, 179-200.